Available online at www.sciencedirect.com
ScienceDirect
Applied Surface Science 254 (2008) 4326–4331
applied surface science
www.elsevier.com/locate/apsusc

The gold and oxygen (3 × 1) structures on W(1 1 2)

Ya.B. Losovyj [a,b,*], Ihor Ketsman [b], N. Lozova [a], John Scott [a], P.A. Dowben [b], I.N. Yakovkin [c], S.M. Zuber [d]

[a] Louisiana State University, CAMD, 6980 Jefferson Highway, 70806 Baton Rouge, LA, USA
[b] Department of Physics and Astronomy and the Nebraska Center for Materials and Nanoscience, 116 Brace Laboratory, P.O. Box 880111, University of Nebraska, Lincoln, NE 68588, USA
[c] Institute of Physics of National Academy of Sciences of Ukraine, Prospect Nauki 46, Kiev 03028, Ukraine
[d] Institute of Experimental Physics, University of Wroclaw, pl. M. Borna 9, Wroclaw, Poland

Available online 19 January 2008

Abstract

The adsorption of two very different adsorbates, gold and oxygen, induce the formation of a (3 × 1) surface structure on both W(1 1 2) and Mo(1 1 2). In spite of similar adsorbate unit cells, the surface electronic structure, derived from photoemission, exhibits pronounced differences for the two adsorbates. Indeed, both experiment and simulations indicate substantial changes in electronic structures of (1 × 1) and (3 × 1) gold overlayers supported by highly anisotropic (1 1 2) plane. We speculate that (3 × 1) is a favored periodicity in the atomic rearrangement of the (1 1 2) surfaces of molybdenum and tungsten due in part as a result of the initial state band structure of these surfaces.

PACS : 68.40-h; 68.35.B-; 68.37.Ef; 31.50.Gh

Keywords: Surface electronic structure of W(1 1 2); Gold; Oxygen; Adsorption; Synchrotron radiation; Photoemission

1. Introduction

The oxidation of chromium, molybdenum and tungsten surfaces have attracted considerable interest because of the various surface oxidation states possible: M_3O, MO_2, M_2O_3 and MO_3 (M = Cr, Mo or W). The stable oxidized surfaces are (perhaps surprisingly) very dependent upon the terminal surface. As expected, oxygen on the low index faces, like the W(1 0 0) surface, have been extensively studied [1–14], but the oxidation of the (1 1 2) plane of W(1 1 2) surface has also attracted attention [14–24]. A number of structural phases at low temperature (e.g. $p(4 \times 1) \rightarrow c(8 \times 2) \rightarrow p(8 \times 1) \rightarrow p(4 \times 1) \rightarrow p(2 \times 2)$) and high temperature (e.g. $p(2 \times 1)$, $p(5 \times 1)$, $p(2 \times 2)$) have been found to occur for oxygen on W(1 0 0), with even an incommensurate (5 × 1) structure [5–8]. The high temperature (3 × 1) and (3 × 3) structure formed during oxida-tion of the W(1 0 0) surface [6,11,12], however, resembles the missing row $p(2 \times 3)$ reconstruction of Mo(1 1 2) which can evolve into a $p(1 \times 3)$ reconstructed MoO_2(0 1 0) surface [25–29].

For W(1 1 2), both gold [10,18] and oxygen [15] will induce a missing row (1 × 3) reconstruction, as we show here. Why the similar surface structures by such different (oxygen and gold) adsorbates? As the electronic structure of the adlayer is so very different with oxygen and gold adsorption, clues to this preferential reconstruction lie in the initial W(1 1 2) band structure.

2. Experimental

The angle-resolved photoemission (ARPES) experiments were performed in an ultra high vacuum described elsewhere [30,31]. These photoemission experiments were done using synchrotron radiation, dispersed by a 3 m toroidal grating monochromator [31], at the Center for Advanced Microstructure and Devices in Baton Rouge, Louisiana [32]. The spectra were taken with photon energy 65 eV at a base pressure of 6×10^{-11} Torr.

* Corresponding author at: Louisiana State University, CAMD, 6980 Jefferson Highway, 70806 Baton Rouge, LA, USA. Tel.: +1 225 578 9373.
E-mail address: ylosovyj@lsu.edu (Y.B. Losovyj).

0169-4332/$ – see front matter © 2008 Elsevier B.V. All rights reserved.
doi:10.1016/j.apsusc.2008.01.064

As with the work undertaken with Mo(1 1 2) [33–35] and clean W(1 1 2) [36], all the angles (both light incidence angles and photoelectron emission angles) reported herein, are with respect to the W(1 1 2) surface normal (the surface Brillouin zone center or SBZ center where the wave vector is parallel with the surface $k_{||} = 0$), while binding energies are reported with respect to the Fermi level. The photoemission spectra were taken with s + p polarized light (45° light incidence angle and the vector potential $\boldsymbol{A}$ residing more in the plane of the surface) with the photoelectrons collected along the surface normal (center of the surface Brillouin zone). The ARPES chamber was equipped with low energy electron diffraction (LEED) and Auger electron spectroscopy (AES). The scanning tunneling microscopy (STM)/LEED experiments were performed in a separate ultra high vacuum chamber using commercial Omicron variable temperature STM apparatus under the same conditions used for the photoemission experiments. Surface cleanness was monitored by AES.

The W(1 1 2) surfaces were prepared using standard methods of flashing and annealing in oxygen [37], resulting in flat, very uniform (1 × 1) furrowed surfaces (Fig. 1) aside from the subsurface defects typical of low index metal surfaces (Fig. 1a). Oxygen exposure is reported in Langmuirs (1 L = 1 × 10^{-6} Torr s). The Au film thickness was determined using stoichiometric $p(1 \times 2)$ structure formation, corresponding to a coverage of 0.5 monolayers, as a fixed reference (benchmark) coverage.

3. Oxygen adsorption on W(1 1 2)

As with Mo(1 1 2) [29,37,38], the initial stages of oxygen exposure to W(1 1 2) are dominated by a $p(1 \times 2)$ structure (Fig. 2b). As we observe this structure starting at coverages well below 0.5 monolayers, the formation of the $p(1 \times 2)$ structure is characterized by growth of adlayer of $p(1 \times 2)$ islands. The $p(1 \times 2)$ structure reaches its stoichiometry at exposures slightly less than 0.5 L.

With increased oxygen exposure, the intensity of main (1 × 1) diffraction spots is enhanced, and at oxygen exposures close to 1 L, the (1 × 1) monolayer structure is formed. Additional exposure to the oxygen leads to formation of the oxygen (4 × 1) structure and then to the (2 × 1) phase, where the latter is complete at ∼1.5 L oxygen exposure (Fig. 2c). Finally, (3 × 1) structure appears with sufficient additional oxygen, gradually supplanting the oxygen (2 × 1) phase as the (3 × 1) domains grow and replace (2 × 1) structure. The

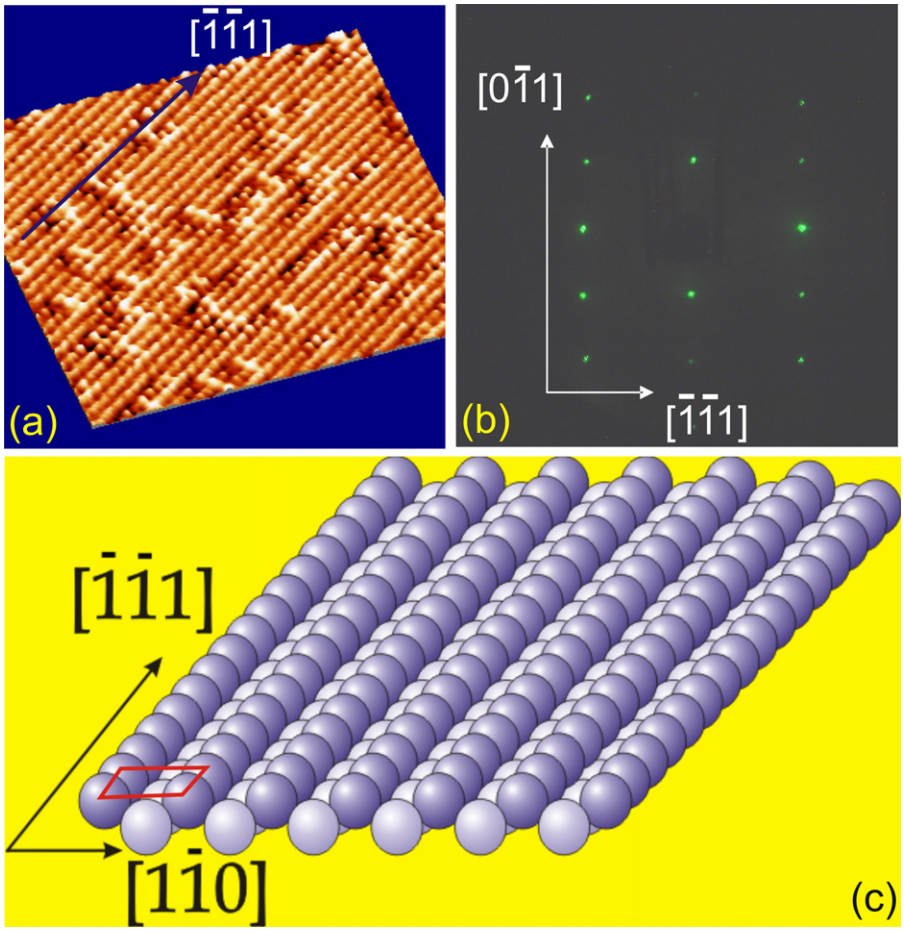

Fig. 1. Furrowed plane of the (1 × 1) terminal surface layer of clean W(1 1 2). (a) STM, (b) LEED pattern taken at 174 eV electron energy and (c) corresponding model for these images. Darker circles represent top-layer of W atoms, light circles represent W atoms in underlying layer. Image (a) is adapted from the issue cover page associated with [36].

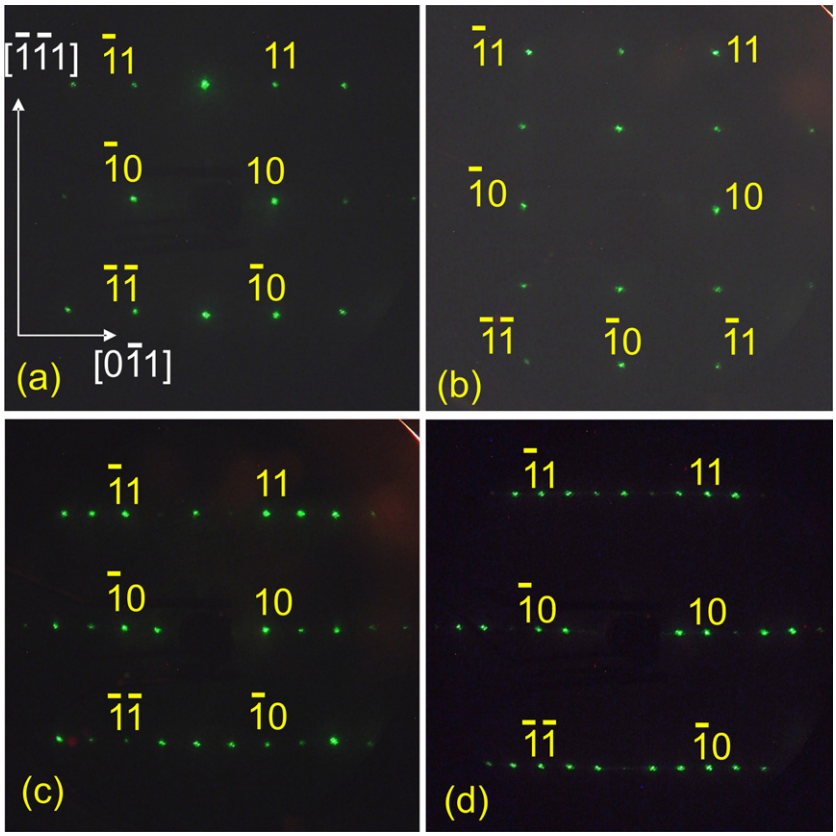

Fig. 2. Typical LEED patterns for oxygen overlayers on W(1 1 2) planes. (a) Clean surface, with an electron energy of 174 eV; (b) $p(1 \times 2)$ structure at 0.5 monolayers or ~0.4 L oxygen, with an electron energy of 93 eV; (c) (2×1) structure at 1.5 monolayers or ~5 L oxygen, with an electron energy of 174 eV and (d) (3×1) structure at 1.66 monolayers or ~12 L oxygen, with an electron energy of 123 eV.

(3×1) oxygen structure is stable up to 18 L oxygen exposures used in our experiments (Fig. 2d). All LEED images reported here (see Fig. 2) were recorded at room temperature after annealing the substrate at 1200 K for each oxygen coverage.

4. Gold adsorption on W(1 1 2)

Gold layers adsorbed on W(1 1 2) form a sequence of adlayer phases that follows that observed for oxygen adsorption, i.e. with increasing gold coverages the surface structures alter in the sequence $p(1 \times 1) \rightarrow p(1 \times 2) \rightarrow p(1 \times 1) \rightarrow p(4 \times 1) \rightarrow p(2 \times 1) \rightarrow p(3 \times 1)$ (see LEED images in the Fig. 3). The scanning tunneling microscopy provides compelling evidence that the Au (3×1) surface structure is a gold bilayer, akin to a missing row reconstruction. Similar structures are also observed with Au adsorption on Mo(1 1 2). Indeed, the Au (3×1) structure on Mo(1 1 2) (Fig. 4a) is not only very close to the calculated (3×1) scanning tunneling microscopy image (Fig. 4b), but nearly identical to the atomic resolution scanning tunneling microscopy images for (3×1) structure on W(1 1 2) substrates (Fig. 4c). Filtered inset in Fig. 4c shows that the paired rows of a (3×1) gold structure on tungsten may consist of linear and zigzag adatoms chains as well as the simple missing row structure, suggesting additional strain in the W(1 1 2) adlayer. Both experimental and calculated STM images do provide the expected lattice constants for such a structure.

5. Comparing oxygen and gold adsorption on W(1 1 2)

At the outset, it is not quite clear why both oxygen and gold should form a sequence of structures on W(1 1 2): $p(1 \times 1) \rightarrow p(1 \times 2) \rightarrow p(1 \times 1) \rightarrow p(4 \times 1) \rightarrow p(2 \times 1) \rightarrow p(3 \times 1)$. It is further surprising, if one considers only the adsorbate, why the (3×1) structure should be so very robust for such very different adsorbates, although oxygen induced reconstructions are well known and even gold low index surfaces are notoriously unstable against reconstructions. The answer lies in the initial state band structure of W(1 1 2). Like Mo(1 1 2) [33–35], there are band crossings for the W(1 1 2) surface 1/3 across the surface Brillouin zone (i.e. with increasing wave vector parallel with the surface $k_{||}$) along $\overline{\Gamma} - \overline{Y}$ [36], as indicated in Fig. 5. The calculated W(1 1 2) surface resonance bands (shown by dashed lines in Fig. 5) have been successfully compared with the experimental band structure extracted from angle-resolved photoemission [36]. Indeed band crossings of the Fermi energy at close to 1/3 along $\overline{\Gamma} - \overline{Y}$ of surface Brillouin zone of W(1 1 2) have very strong surface weight [36] which makes this surface very susceptible to a (3×1) reconstruction, if there is an accompanying decrease in

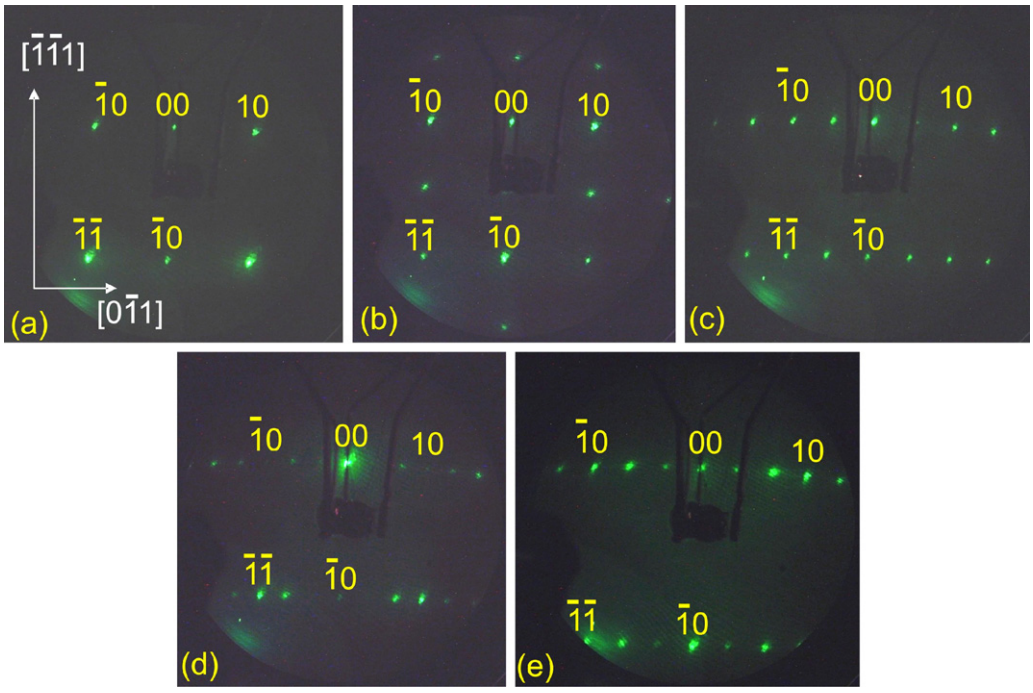

Fig. 3. Typical LEED patterns for Au adlayers on W(1 1 2) planes. (a) Clean surface, with an electron energy of 83 eV; (b) $p(1 \times 2)$ structure at 0.5 monolayers, with an electron energy of 83 eV; (c) (2×1) structure at 1.5 monolayers with an electron energy of 87 eV; (d) (3×1) structure at 1.66 monolayers with an electron energy of 87 eV and with (e) an electron energy of 51 eV.

the electron density at the Fermi level. This is seen to occur for both gold and oxygen adsorption.

The photoemission spectra taken for gold (right panel of Fig. 6) and oxygen (left panel of Fig. 6) show gradual changes in valence band region when the adsorbate coverage increases.

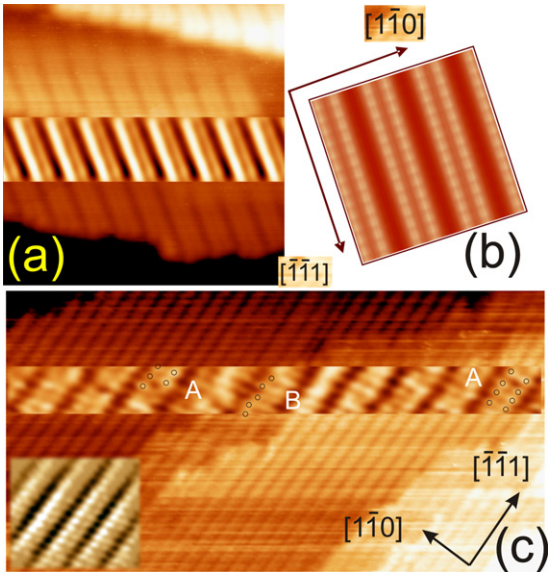

Fig. 4. Experimental (a, c) and simulated (b) STM images for (3×1) and (1×1) Au overlayers on Mo and W surfaces. (a) 14.6 nm × 14.6 nm STM image of (3×1) Au/Mo(1 1 2) with 12.5 nm × 2.8 nm inset after fast Fourier transform (FFT) filtering; (b) calculated STM image of (3×1) gold layer on Mo(1 1 2) and (c) 56.6 nm × 29.2 nm image of (3×1) Au structure on W(1 1 2), middle 22.3 nm × 1.9 nm inset after derivative filtering, left bottom 6.8 nm × 5.8 nm inset after FFT.

Gold deposition (left panel) leads to the addition of strong gold d-band features that shift towards higher binding energies and suppress tungsten valence bands features with increasing gold coverages. Tungsten bands are still visible up to 1.5 monolayer but the density of states near to E_F is quickly suppressed (Fig. 6). The (3×1) Au structure on W(1 1 0) exhibits photoemission spectra (spectra 4 in Fig. 6, right panel) that closely resembles the "bulk" gold valence band structure and can be considered as physical Au monolayer which consists of a bilayer with a (1×1) first layer structure and paired gold rows in second layer on the top, running along [1 1 1] direction, with empty row in between, based upon the STM and LEED evidence discussed above. We notice substantial difference of this valence band structure from that corresponding to (1×1) Au adlayer.

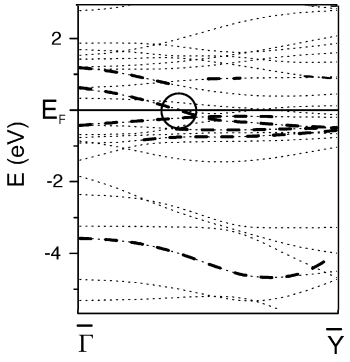

Fig. 5. Surface bands calculated along the $\overline{\Gamma} - \overline{Y}$ high symmetry line of the surface Brillouin zone for a seven-layer slab representing the W(1 1 2) surface. The calculated W(1 1 2) surface resonance bands are shown by dashed lines. The key Fermi level crossing is encircled as described elsewhere [36].

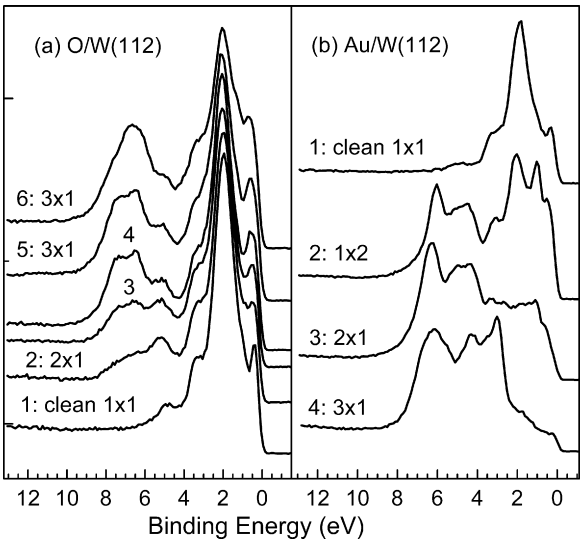

Fig. 6. Photoemission spectra taken with 65 eV photon energy at the normal emission geometry for several coverages of (a) oxygen (left panel) and (b) gold (right panel) on W(1 1 2). (a) Left panel – oxygen coverages 1, 0; 2, 1.35 L; 3, 2 L; 4, 4 L; 5, 6 L and 6, 12 L. For (b) right panel – gold on W(1 1 2) 1, clean; 2, structure $p(1 \times 2)$, $T_{an} = 1350$ K; 3, structure (2×1) $T_{an} = 1200$ K and 4, structure (3×1) $T_{an} = 1200$ K.

Oxygen influence on W(1 1 2) (see right panel, Fig. 6) seems to affect the substrate electronic structure much less than gold, but again, the lowest occupied W(1 1 2) band is shifted away from the Fermi level, with an increase in the adlayer oxygen 2p bands at 6–8 eV binding energy. The suppression of tungsten surface state near Fermi level (spectrum 2, left panel) along with a slight shift of the tungsten features towards higher binding energies is certainly consistent with a reduction of the surface density of states near the Fermi level.

6. Conclusions

In spite of closely similar adsorbate (3×1) unit cells for gold and oxygen on W(1 1 2) the surface electronic structures derived from the synchrotron based ARUPS experiments exhibit pronounced differences. Nonetheless, both share a common connection in that there is a decrease in the density of states near the Fermi level with increased adsorbate coverages.

In this context, it is also possible to understand why Mo(1 1 2) favors $(3 \times n)$ reconstructions (e.g. (3×3), (3×1) adlayer structures). As suggested elsewhere [35], Mo(1 1 2) surface reconstructures are also dominated by the Fermi level band crossings and given that W(1 1 2) and Mo(1 1 2) have similar band structure near the Fermi level, the tendency towards similar reconstructions should not be so very surprising. Comparing adsorbates that act as reducing agents with adsorbates that act as oxidizing agents, we can anticipate that the adsorption sites should differ, although constrained by geometric effects, and the bonding to the surface frontier orbitals, which will affect the symmetry of the adsorbation site. While (3×1) surface reconstruction will be favored, the details of the surface structure may differ substantially. Neglecting the affect of the surface and adsorbate frontier orbitals, if there is to be a reduction in the total surface energy, by shifting the density of states in the surface electronic structure away from the Fermi level, adsorbates that tend towards oxidation should favor the (3×1) sites where electron pooling occurs, and adsorbates that favor reduction should favor (3×1) sites that have lower electron density.

Acknowledgements

The support of by IFD University of Wroclaw within framework of project no. 2016/W/IFD2003, the NSF "QSPINS" MRSEC (DMR 0213808), and the Nebraska Research Initiative at the University of Nebraska are gratefully acknowledged. The Center for Advanced Microstructures and Devices is supported by the Louisiana Board of Regents. We also thank S. Mroz, A. Ciszewski and Z. Szczudlo for interest and help during the course of the various the STM experiments and Josef Hormes for his support for the photoemission measurements.

References

[1] P.J. Estrup, Surf. Sci. 299–300 (1994) 722.
[2] P.F. Lyman, D.R. Mullins, Phys. Rev. B 51 (1995) 13623.
[3] Ch. Park, H.M. Kramer, E. Bauer, Surf. Sci. 115 (1982) 1.
[4] C. Park, H.M. Kramer, E. Bauer, Surf. Sci. 116 (1982) 467.
[5] H.M. Kramer, E. Bauer, Surf. Sci. 92 (1980) 53.
[6] E. Bauer, H. Poppa, Y. Viswanath, Surf. Sci. 58 (1976) 517.
[7] M.S. Altman, E. Bauer, Surf. Sci. 347 (1996) 265.
[8] H. Yamazaki, T. Kamisawa, T. Kokubun, T. Haga, S. Kamimizu, S. Sakamoto, Surf. Sci. 477 (2001) 174.
[9] J.A. Meyer, Y. Kuk, P.J. Estrup, P.J. Silverman, Phys. Rev. B 44 (1991) 9104.
[10] P. Alnoty, D.J. Auerbach, J. Behm, C.R. Brundle, A. Viescas, Surf. Sci. 213 (1989) 1.
[11] N. Moslemzadeh, S.D. Barrett, Surf. Sci. 600 (2006) 2299.
[12] S. Murphy, G. Manai, I.V. Shvets, Surf. Sci. 579 (2005) 65.
[13] V.P. Ivanov, A.N. Goldobin, V.N. Kolomiichuk, V.I. Savchenko, Soviet Phys. Solid State 16 (1974) 240.
[14] L.L. Han, C.L. Liu, Z.X. Wang, Z.Y. Diao, Chin. J. Catalysis 26 (2005) 707.
[15] C.C. Chang, L.G. Germer, Surf. Sci. 8 (1967) 115.
[16] C.C. Chang, Surf. Sci. 8 (1967) 115.
[17] G.C. Wang, Phys. Rev. B 28 (1983) 6795.
[18] J. Kolaczkiewicz, E. Bauer, Surf. Sci. 144 (1984) 477.
[19] B.A. Chuikov, V.D. Osovskii, Yu.G. Ptushinskii, V.G. Sukretnyi, Surf. Sci. 213 (1989) 359.
[20] B.J. Hopkins, G.D. Watts, Surf. Sci. 44 (1974) 237.
[21] G.-C. Wang, T.-M. Lu, Phys. Rev. B 28 (1983) 6795.
[22] H. Bu, O. Grizzi, M. Shi, J.W. Rabalais, Phys. Rev. B 40 (1989) 10147.
[23] I.N. Yakovkin, Surf. Sci. 577 (2005) 229.
[24] A. Kiejna, Phys. Rev. B 74 (2006) 235429.
[25] T. Schroeder, J.B. Giorgi, A. Hammoudeh, N. Magg, M. Baumer, H.-J. Freund, Phys. Rev. B (2002) 115411.
[26] T. Schroeder, J. Zegenhagen, N. Magg, B. Immaraporn, H.-J. Freund, Surf. Sci. 552 (2004) 85.
[27] A.K. Santra, B.K. Min, D.W. Goodman, Surf. Sci. 513 (2002) L441.
[28] A. Kiejna, R.M. Nieminen, J. Chem. Phys. 122 (2005), 044712.
[29] M. Sierka, T.K. Todorova, J. Sauer, S. Kaya, D. Stacchiola, J. Weissenrieder, S. Shaikhutdinov, H.-J. Freund, J. Chem. Phys. 126 (2007) 234710.
[30] P.A. Dowben, D. LaGraffe, M. Onellion, J. Phys. Condens. Matter 1 (1989) 6571.
[31] Ya.B. Losovyj, I. Ketsman, E. Morikawa, Z. Wang, J. Tang, P.A. Dowben, Nucl. Instrum. Methods Phys. Res. A 582 (2007) 264.
[32] J. Hormes, J.D. Scott, V.P. Suller, Synchrotron Radiat. News 19 (2006) 27.

[33] I.N. Yakovkin, J. Zhang, P.A. Dowben, Phys. Rev. B 63 (2001) 11540.
[34] H.-K. Jeong, T. Komesu, I.N. Yakovkin, P.A. Dowben, Surf. Sci. Lett. 494 (2001) L773.
[35] T. McAvoy, J. Zhang, C. Waldfried, D.N. McIlroy, P.A. Dowben, O. Zeybek, T. Bertrams, S.D. Barrett, Eur. Phys. J. B 14 (2000) 747.
[36] Ya.B. Losovyj, I.N. Yakovkin, J.H.K. Leong, P.A. Dowben, Phys. Stat. Sol. (b) 241 (2004) 829.
[37] T. Aruga, K. Taleno, K. Fukuri, Y. Iwasawa, Surf. Sci. 324 (1995) 17.
[38] T. Sasaki, Y. Goto, R. Tero, K. Fukui, Y. Iwasawa, Surf. Sci. 502 (2002) 136.